# Effect of Obstacle Spacing on Flame Acceleration and DDT in Obstructed Channels

**Vadim N. Gamezo[1], Takanobu Ogawa[2], and Elaine S. Oran[1]**

[1]Laboratory for Computational Physics and Fluid Dynamics,
Naval Research Laboratory, Washington, DC 20375

[2]Department of Mechanical Engineering, Seikei University,
Kichijoji-Kitamachi, Musashino-shi, Tokyo, 180-8633, Japan

Deflagration-to-detonation transition (DDT) in practical systems is a complicated combination of several multiscale physical phenomena that occur in three consecutive stages [1]: (1) the evolution of flame and flow that creates conditions for detonation initiation, (2) the actual formation of the detonation wave, and (3) the spread of the detonation into large areas of unburned material that ensures the detonation survival. Channels with obstacles provide a controlled experimental environment in which all three stages of DDT can be observed and studied in detail. In our previous work [2], we successfully modeled this type of experiments and reproduced the main regimes of flame propagation observed in obstructed channels: supersonic turbulent flames, quasi-detonations, and detonations. In this paper, we study the flame acceleration and DDT phenomena for different obstacle spacings, consider stochastic properties of DDT, and analyze the effect of imposed symmetry.

The numerical model is based on reactive Navier-Stokes equations solved on a dynamically adapting Cartesian structured mesh using an explicit, second-order, Godunov-type numerical scheme incorporating a Riemann solver. The energy release is described by a one-step Arrhenuis kinetics. The reactive system parameters approximately correspond to the stoichiometric $H_2$-air mixture at 1 atm and 293 K with the laminar flame thickness 0.035 cm and the laminar flame velocity 3 m/s. The reactive system and the numerical model are described in more detail in [2]. Computations were performed for the minimum computational cell size $dx_{min} = 1/128$, $1/256$, or $1/512$ cm, as discussed below.

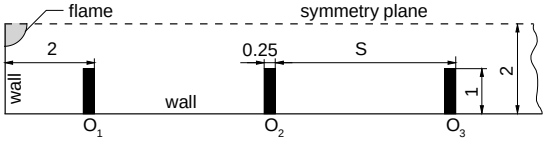


**Fig. 1.** Computational setup. Obstacles $O_1, O_2, ...O_n$ are evenly spaced along the whole channel length. Walls and obstacle surfaces are adiabatic no-slip reflecting boundaries. Sizes are in centimeters. Initial flame radius is 0.5 cm.

We consider a two-dimensional (2D) channel $2 \times 128$ cm with uniformly spaced obstacles placed at the bottom wall, as shown in Fig. 1. The channel is closed at the left end and filled with the stoichiometric $H_2$-air mixture. To ignite the flame, we initially place a circular region of hot burned material at the left wall and add external energy to the burned region. The energy added per unit mass is 25 times larger than the chemical energy. This models a spark ignition powerful enough to create a strong shock.

The flame and flow development for a very similar configuration with $S$=4 cm was described in detail in [2]. The only difference is that here we use the spark ignition generating initial shocks and causing fast expansion of the initial burned region that quickly spreads past the first obstacle. The subsequent flame and flow acceleration is very similar to that described in [2], and is closely related to the increase in the total burning rate in the system. Analysis of simulation results shows several mechanisms responsible for the burning rate increase, most of them related to the growth of the flame surface area.

**Correspondence to : gamezo @ lcp.nrl.navy.mil** 

At initial stages, the flame surface increases as the leading edge of the flame propagates with the fast flow along the symmetry plane and leaves unburned material in the lower part of the channel between obstacles. This forms an extended "reaction zone" that spreads over several obstacle spacings, but eventually stabilizes because the material far behind the leading flame front burns out. The flame surface area increases significantly when the flame interacts with shear layers and recirculation flow in wake of obstacles. As the flame passes obstacles, it also wrinkles due to the Rayleigh-Taylor instability caused by the flow acceleration. Another mechanism for the flame surface increase involves shock-flame interactions that trigger Richtmyer-Meshkov instabilities. Strong shocks produced by the ignition pulse decay quickly, but then strengthen again because of the flame acceleration. The elevated temperature behind shocks also contributes to the increased burning rate.

As the shock and the flame accelerate, the leading edge of the flame remains about 1 cm behind the leading shock, which diffracts at every obstacle and reflects from the bottom wall after each diffraction. The type of shock reflection changes from regular to strong as the reflection point approaches the next obstacle. The resulting Mach stem becomes stronger after each diffraction, and eventually a collision of the Mach stem with an obstacle ignites a detonation.

Results of similar computations for $S$=1, 1.5, 2, 3, 4, 6, and 8 cm, summarized in Figs. 2 and 3, show two main effects of obstacle spacing. First, the flame acceleration increases when $S$ decreases (as shown by different slopes of curves in Fig. 3) because more obstacles per unit length create more perturbations that increase the flame surface area more quickly. Second, DDT occurs more easily when the obstacle spacing allows Mach stems to form. These two effects are responsible for three different regimes of flame acceleration and DDT observed in our simulations:

Regime (1): Detonation is ignited when a Mach stem formed by the diffracting shock reflecting from the bottom wall collides with an obstacle. We observe this for $S$=8, 6, and 4 cm, as shown in Figs. 2 and 3. The detonation appears earlier for smaller $S$ mostly because the flame accelerates more quickly when there are more obstacles. The detonation initiation is also affected by the strength of the Mach stem, which expands and weakens for larger $S$, as shown in Fig. 2. As a result, the average flame velocity just before DDT increases with $S$ and equals 825, 880, and 925 m/s for $S$=4, 6, and 8, respectively.

Regime (2): Mach stems do not form and there is no DDT within the channel length, as shown in Figs. 2 and 3 for $S$=3, 2 and 1.5 cm. Without Mach stems, collisions of shocks with obstacles produce weaker reflected shocks that are not strong enough to ignite a detonation. There is no noticeable flame acceleration in the second half of the channel, where the flame propagates at 850, 890, and 1000 m/s for $S$=2, 3, and 1.5, respectively. A detonation would probably never be ignited even in longer channels.

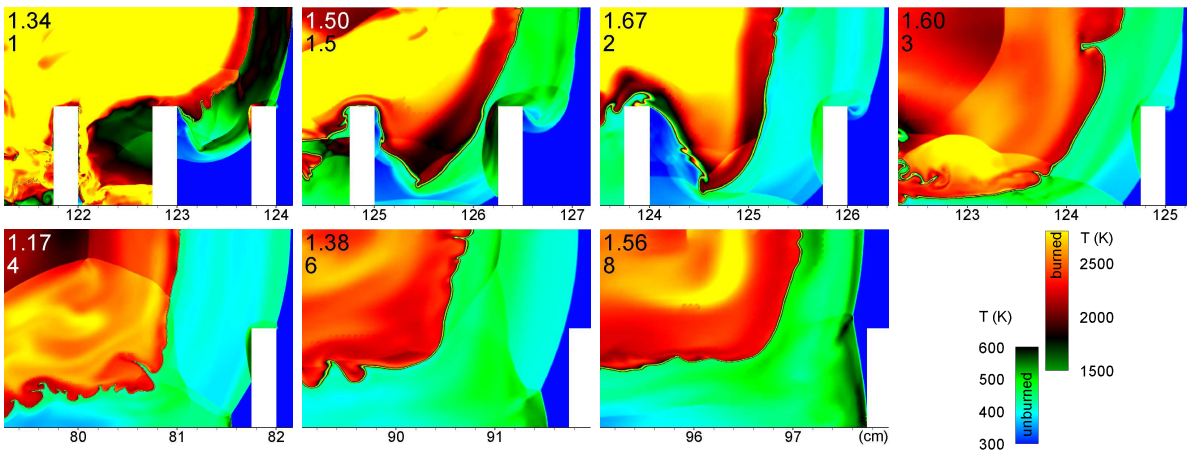


**Fig. 2.** Flame and shock configurations just before the detonation initiation ($S$=1, 4, 6, 8) or at the end of the channel ($S$=1.5, 2, 3). Time in milliseconds and $S$ in centimeters are shown in frame corners. $dx_{min}$=1/512 cm ($S$=1, 4) or 1/128 cm ($S$=1.5, 2, 3, 6, 8).

Regime (3): Detonation is ignited by a direct collision of the leading shock with the top part of the obstacle, as shown in Fig. 2 for $S$=1 cm. Because this collision does not produce a Mach stem, the ignition requires a much stronger leading shock, and therefore a significantly faster flame, than for the Regime (1). This additional flame and shock acceleration is provided by a series of detonations that occur in isolated pockets of unburned material between obstacles behind the leading flame front. Times and locations of these detonations are shown by points in Fig. 3. These isolated detonations usually form after multiple shock reflections and shock-flame interactions near the bottom wall. They do not reach the leading edge of the flame but generate strong shocks, increase the total burning rate, and thus contribute to the leading shock strength. Isolated detonations appear more often as the flame speed and the shock strength increase. The actual DDT occurs when the average flame speed reaches 1200 m/s.

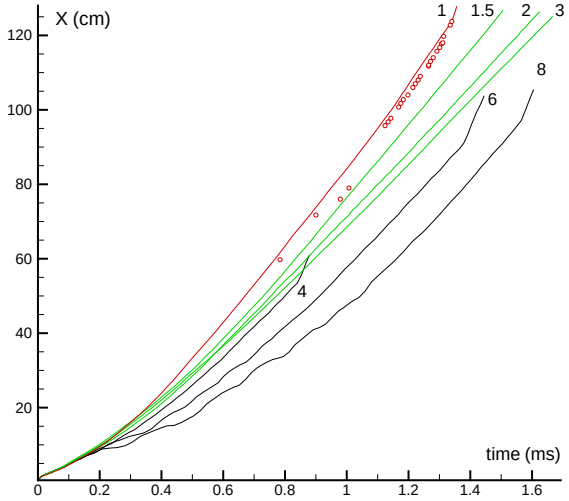


**Fig. 3.** Position of leading edge of flame as function of time computed for $S$=1-8 cm. Points indicate times and locations of isolated detonations behind the leading flame front for $S$=1. Colors correspond to different regimes. $dx_{min}$=1/512 cm ($S$=1) or 1/128 cm ($S$=1.5-8). Sharp increase in slope indicates transition to detonation (occurs for black and red curves).

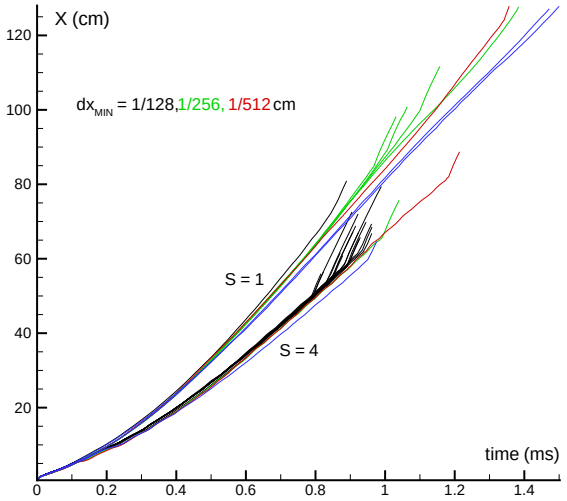


**Fig. 4.** Flame position as function of time computed for $S$=1 and 4 cm for different numerical resolutions. Multiple green and black lines were computed for slightly different initial temperatures to show the stochasticity effect. Blue lines ($S$=1, $dx_{min}$=1/128, 1/256 cm, and $S$=4, $dx_{min}$=1/128 cm) correspond to full 4×128 cm channels with two symmetrical sets of obstacles.

To study the effect of numerical resolution on the results discussed here, we considered two cases, $S$=4 and $S$=1, that represent two different regimes of DDT. The results obtained for $dx_{min}$=1/128, 1/256, and 1/512 cm are shown in Fig. 4 by black, green, and red lines, respectively. Because our computations involve multiple stochastic phenomena, the effect of numerical resolution cannot be properly evaluated without estimating the dispersion of the results related to stochastic properties of the system. To estimate the stochastic dispersion, we computed two cases multiple times varying the initial temperature within 0.01 K interval, which is too small to have systematic effects. The results are shown by multiple black ($S$=4, $dx_{min}$=1/128) and green ($S$=1, $dx_{min}$=1/256) lines in Fig. 4.

For $S$=4, represents the Regime (1) where DDT is controlled by Mach stems, the flame acceleration is practically independent of the numerical resolution, though the detonation tends to appear later as the resolution increases. For example, the DDT time 1.18 ms observed for $dx_{min}$=1/512 is significantly longer than 0.79-0.93 ms obtained in multiple computations for $dx_{min}$=1/128. A detailed analysis of the high-resolution computation shows, however, that detonations appear in the system six times between 0.71 and 1.13 ms, but do not reach the leading edge of the flame. In two cases, at 0.894 ms and 0.940 ms, detonations almost survive. If the flame configuration at the time of DDT was only a little different (which is possible in a stochastic system), these detonations could survive. This indicates that the dispersion interval for $dx_{min}$=1/512 extends down at least to 0.894 ms and overlaps with the dispersion

interval for $dx_{min}$=1/128. In any case, the DDT time for $S$=4 is well below 1.37 ms observed for $S$=6 (Fig. 3), and our conclusions about the effect of obstacle spacing on Regime (1) are still valid.

The effect of numerical resolution on Regime (3) is more pronounced, as shown in Fig. 4 for $S$=1. The black line computed for $dx_{min}$=1/128 shows higher flame acceleration and significantly shorter DDT time compared to higher-resolution computations. Even though the DDT mechanism is still the same, we consider this low resolution inadequate for Regime (3). The stochasticity test performed for the medium resolution ($dx_{min}$=1/256) shows the dispersion of DDT times between 0.97 and 1.39 ms (see four green lines in Fig. 4). Three of the cases computed produced DDT between 0.97 and 1.1 ms. The fourth case shows a similar flame acceleration up to 1 ms, then the flame slows down until 1.15 ms, and accelerates again to produce DDT at the last obstacle at 1.39 ms. The high-resolution case (red line, $dx_{min}$=1/512) shows a similar flame acceleration up to 0.8 ms, after which the flame speed continues to increase more gradually than for $dx_{min}$=1/256. DDT for $dx_{min}$=1/512 occurs at 1.34 ms, within the dispersion interval for $dx_{min}$=1/256. Medium and high resolutions show a reasonable convergence for the Regime (3), and we consider them adequate for the numerical analysis of this regime.

The geometry shown in Fig. 1 can be considered as a half of a larger channel with two sets of obstacles symmetrically placed at top and bottom walls, or as the actual channel with only one set of obstacles at the bottom. Both half-channel and full-channel configurations can be realized in experiments or computations, and it is not evident whether these two configurations should produce the same results. To study this issue, we repeated the simulations for $S$=4 and $S$=1 using the full channel (4x128 cm) configuration. The results are shown by blue lines in Fig. 4. Because here we ignore possible influence of heat losses and viscous boundary layer at the top wall for the half-channel, the difference between the half-channel and full-channel simulations is attributed only to the effect of imposed symmetry.

For $S$=4 this effect is rather small. The flame accelerates a little faster in the half-channel, probably because ideally symmetrical shock reflections at the top wall (symmetry plane) generate slightly stronger shocks that interact with the flame and eventually contribute to the leading shock strength. The detonation in the full channel appears near the same obstacle $O_{15}$ as in several half-channel computations.

For $S$=1, there is a significant difference between results obtained in full and half-channels. In the full channel, the flame accelerates more slowly, and the leading shock never becomes strong enough to ignite a detonation on a direct collision with an obstacle. There is no DDT within the channel length, and it is unlikely that a detonation would appear in a longer channel because the flame does not accelerate after 90 cm and even slows down. Full-channel computations give practically the same result for two different numerical resolutions ($dx_{min}$=1/128 and 1/256), as shown by two blue lines for $S$=1 in Fig. 4.

The strong effect of imposed symmetry for $S$=1 is related to isolated detonations behind the leading flame front that are critical for final stages of flame acceleration in this regime. In a half-channel, each of these detonations implies a symmetric explosion at the opposite wall. Strong shocks produced by isolated detonations reflect from the symmetry plane and increase the probability of subsequent isolated detonations in neighboring locations. In a full channel, these detonations appear at random times and locations near the top or bottom wall. The lack of synchronized explosions and symmetrical shock reflections reduces maximum pressures generated by shock collisions. As a result, isolated detonations do not appear often enough to accelerate the flame. We observe this effect in numerical simulations, but this is a physical phenomenon that can also occur in experiments with full and half-channels.

**Acknowledgments.** This work was supported in part by Japanese New Energy and Industrial Technology Development Organization (NEDO) in cooperation with Shumizu Corporation, the NASA ATP program, and by the Naval Research Laboratory (NRL) through the Office of Naval Research. Computing facilities were provided by the DOD HPCMP program.

**References**

1. E. S. Oran and V. N. Gamezo. *Combust. Flame* **148**, 4 (2007)
2. V. N. Gamezo, T. Ogawa, and E. S. Oran. *Proc. Combust. Inst.* **31** (2007)